

# Johnstown

Monomict Brecciated Diogenite, 40.3 kg

*Seen to fall*



**Figure 1:** Slab through a piece of Johnstown, showing the coarse pyroxene texture. Width of sample is approximately 5 cm. Photo by D. Ball, ASU School of Earth and Space Exploration.

**Introduction:** The Johnstown diogenite (**Figure 1,2**) fell at 4:20 PM in western Weld County, Colorado, USA, on July 6, 1924, after local residents heard “four terrific explosions” followed by a number of minor tremors (Hovey, 1925). At least four of the fragments were seen to fall (including one that fell next to a funeral service at a local church), and the total area over which the fall occurred (**Figure 3**) describes an ellipse ten miles long and two miles wide, elongated SSW-NNE, with individual stone size increasing to the NNE (Hovey, 1925). Hovey (1925) gives the location (latitude and longitude) and weight for 26 recovered stones, weighing 40.3 kg in total, far exceeding the total weight of all other recovered diogenites (Mason and Jarosewich, 1971). The largest individual stone, which weighed 23.5 kg at the time of the fall, is currently housed at the American Museum of Natural History in New York; its current weight, however, is only 17 kg (Hovey, 1925; Grady, 2000). Other remaining pieces of the meteorite are housed at the Denver Museum of Natural History (5.2 kg), Arizona State University (2.48 kg), and the Chicago Field Museum (177 g) (Grady, 2000).

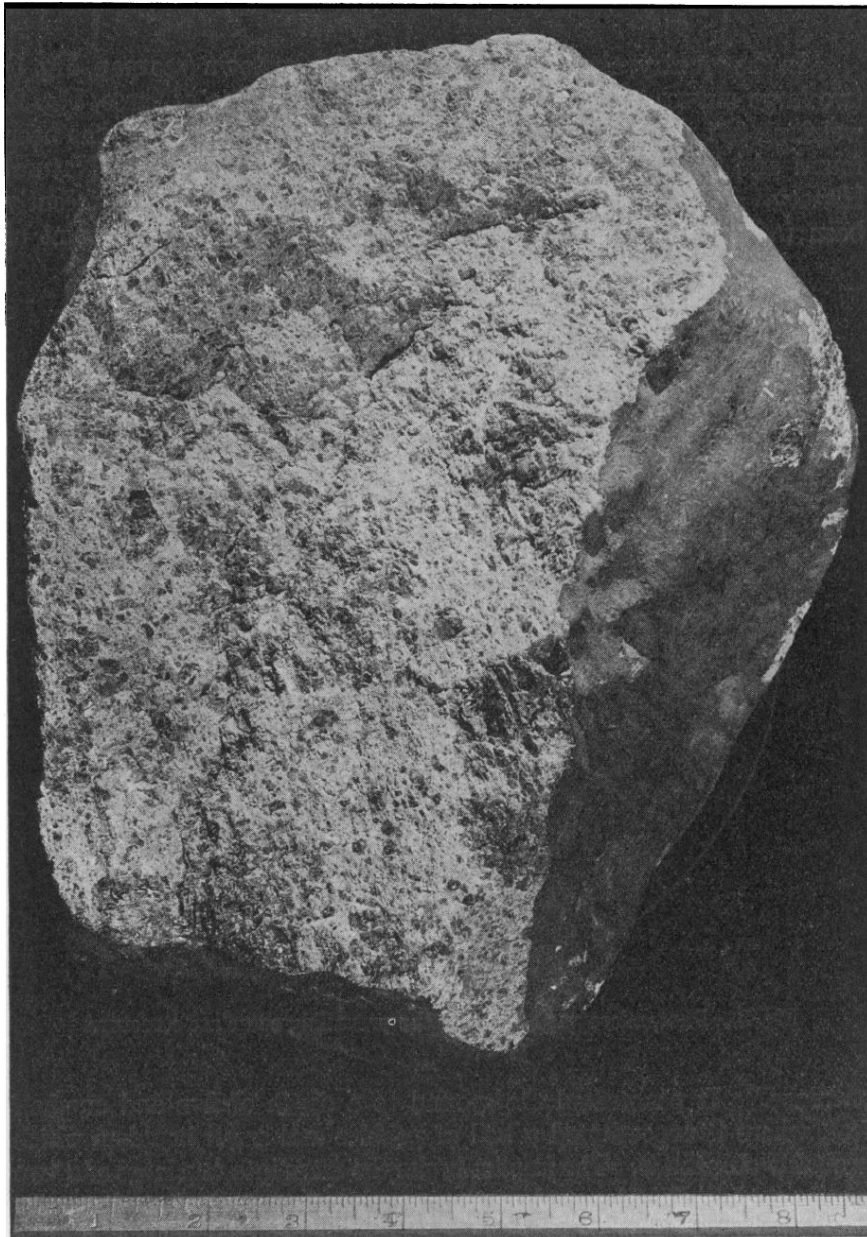


**Figure 2:** The largest recovered fragment of the Johnstown meteorite. Hovey (1925), Figure 2.

As can be seen in **Figure 1 and 2**, the Johnstown meteorite has a noticeable fusion crust; like other diogenites, it is dominated by porphyritic Mg-rich pyroxene phenocrysts, with some iron-rich pyroxene occurring as overgrowths on other phenocrysts and groundmass phases, and mesostasis glass (Genge and Grady, 1999). The major element chemistry of the fusion crust (analyzed by Genge and Grady, 1999) is shown in **Table 2**. An analysis of heavy cosmic-ray fission tracks suggested an original, pre-atmospheric radius of  $\geq 27$  cm for Johnstown (Fleischer et al, 1967b).

Johnstown is a monomict brecciated diogenite; its chemistry and texture are similar to terrestrial ultramafic cumulates, showing coarse-grained

clasts of recrystallized orthopyroxene in a fine-grained matrix of the same chemical constituents.

**Petrography:** Johnstown was first described in detail by Hovey (1925); as he died before completing preliminary work on the meteorite, his analysis was published with supplemental information and chemical analyses by Merrill and Shannon (in the same work). Other basic petrographic and mineralogic descriptions are contained in Mason (1963a) and Floran et al (1981).

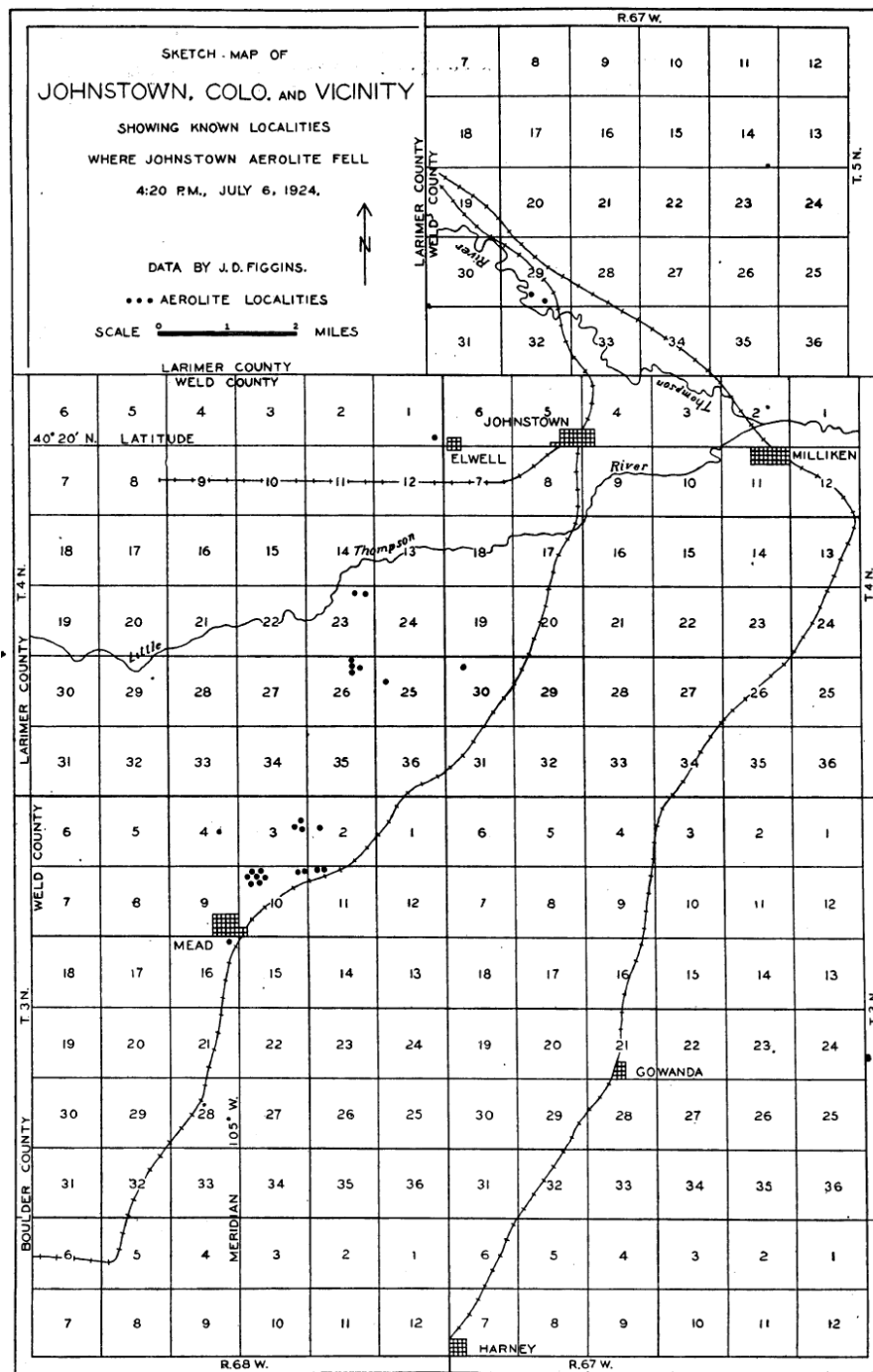


**Figure 3:** Hovey (1925) map of Weld County, Colorado; the black dots mark locations where pieces of the Johnstown meteorite were recovered. The two dots along the Thompson River, north of Johnstown, mark the largest recovered pieces, including the fragment seen in Figure 2.

Johnstown is an ultramafic breccia composed of mostly (>95% modal) greenish-gray, coarse-grained, cm-sized, angular to subrounded orthopyroxene and orthopyroxenite clasts (Floran et al, 1981), in a brecciated, comminuted, fine-grained orthopyroxenite matrix (Figure 4) with some interstitial, twinned, inclusion-free plagioclase feldspar (Figure 5). While the clasts are poorly sorted, and can be of an extremely variable size range (Floran et al, 1981), clasts of up to 5-7 cm have been reported in the literature (Merrill and Shannon *in Hovey*, 1925; Mason, 1963a; Floran et al, 1981), and clasts greater than 1 cm contain multiple recrystallized orthopyroxene grains in contact with each other, i.e., orthopyroxenite (Floran et al, 1981), suggestive of recrystallization followed by brecciation from the original coarse-grained, igneous, cumulate texture.

The orthopyroxenes contain numerous fractures (Floran et al, 1981), exhibit undulatory extinction (Mason, 1963a; Floran et al, 1981), have exsolution lamellae (Mason, 1963a; Mori and Takeda, 1981a;

Molin et al, 1991), exhibit 120° triple-grain boundaries (Floran et al, 1981), and contain numerous opaque and silicate-bearing inclusions (Merrill and Shannon *in Hovey*, 1925; Floran et al, 1981), many of which are oriented in a planar orientation (Gooley and Moore, 1976; Mori and Takeda, 1981a).

Besides orthopyroxene, plagioclase feldspar, and clinopyroxene (as lamellae and inclusions in orthopyroxene), other accessory phases in Johnstown include clinopyroxene (as distinct grains in the matrix), chromite, troilite and other sulfide minerals, free metal, tridymite, olivine, and phosphates; their modal amounts are shown in **Table 1**. (Note: phosphates were *not* identified by Bowman et al (1997), but were identified in the same two thin sections by Bowman et al (1996), so I have included them here.)

**Table 1:** Modal analyses of the Johnstown diogenite.

reference	Merrill and Shannon	Merrill and Shannon	Mason	Mason and Jarosewich	Bowman et al	Bowman et al
	<i>in Hovey</i> 25	<i>in Hovey</i> 25	63	71	97	97
type	mode	norm	mode	mode	mode1	mode2
opx	>95	69	96	95.8	95.9	95.4
cpx	--	2.9	--	--	0.5	0.5
plagioclase	0.7	10.56	0.7	3	0.1	1
tridymite	--	--	--	--	0.4	0.6
olivine	--	16.73	--	--	0	0
troilite	--	--	<1	1.2	2.8	2.3
chromite	--	--	<2	<0.1	0.1	0.1
metal	0.33	--	0.35	0.3	0.2	0.2
phosphate	--	--	--	--	<0.01	<0.01

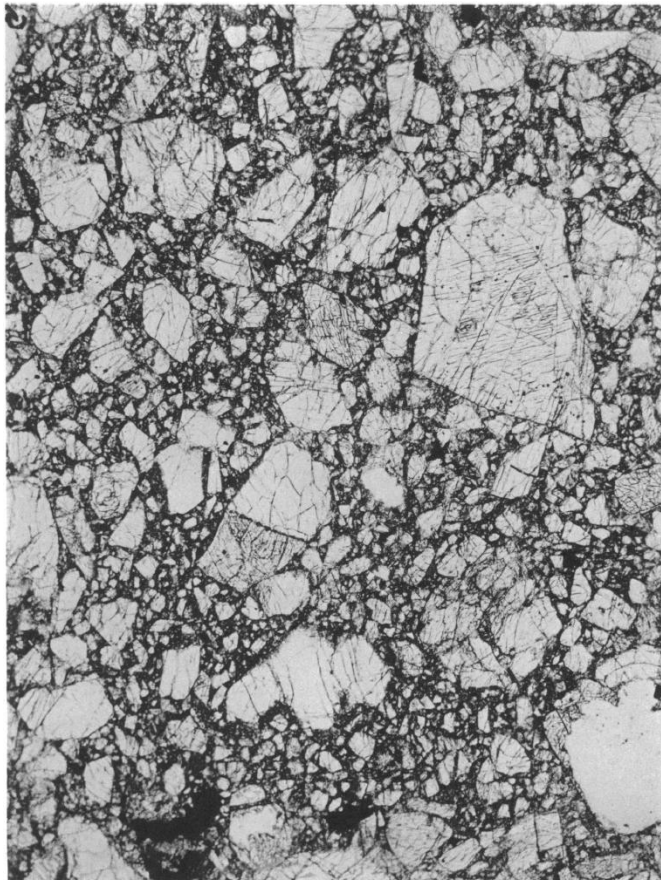


**Figure 4:** Thin-section photomicrograph of the Johnstown meteorite, showing large fragments of orthopyroxene in a brecciated groundmass of the same mineralogy. Mason (1963a), Figure 1. No scale given.

A clarification of the Merrill and Shannon (*in Hovey*, 1925) normative mineralogy in **Table 1** is necessary at this point; Merrill and Shannon themselves pointed out that their Johnstown samples contained no olivine, and a brief discussion of diogenite norms contained in

Mason (1963a) explains that the normative calculation will always overstate olivine in these meteorites, as  $\text{Al}_2\text{O}_3$  and  $\text{CaO}$  are assigned to plagioclase (which is also



**Figure 5:** Interstitial plagioclase (marked with a “1”) in a slightly crushed portion of Johnstown, with angular and subrounded orthopyroxene (“2”). Figure 5 from Merrill and Shannon, in Hovey, 1925. No scale given.

overestimated) when they are largely found in pyroxene, leaving excess  $\text{FeO}$ ,  $\text{MgO}$ , and  $\text{SiO}_2$  that the normative calculation assigns to olivine. (An important note: Floran et al (1981) reported a single crystal of olivine in Johnstown, so it is not entirely absent.)

Equilibration temperatures for Johnstown, based on two-pyroxene and pyroxene-spinel thermometry, have been recently calculated in

the 640-650°C range (Mittlefehldt, 1994a). This is in agreement with previous work by the orthopyroxene-spinel thermometer used by Mukherjee and Viswanath (1987), who calculated equilibration temperature of 687°C, and Miyamoto et al (1975), who noted that the highly-ordered Mg-Fe distribution between the M1 and M2 sites in Johnstown orthopyroxenes suggested slow cooling and equilibration in the 500-700°C range.

The degree of brecciation in Johnstown is rather variable; Floran et al (1981) reported heavily brecciated zones abutted against nearly unbrecciated or slightly brecciated areas of the rock, suggesting a complicated but overall low-level shock history.

### **Mineral Chemistry:**

**Pyroxene:** Johnstown pyroxenes are nearly all hypersthene, with clinopyroxene manifested in three ways: (1) as exsolution lamellae in orthopyroxene (see below), (2) as diopside in metal-rich inclusions in orthopyroxene (Sideras et al, 2004), and (3) as anhedral, 40  $\mu\text{m}$  grains of diopside associated with coarse patches of opaques and tridymite in the matrix (Floran et al, 1981). Orthopyroxene compositions taken from the available literature, though somewhat variable, are centered around  $\text{Wo}_{2.5}\text{En}_{73}\text{Fs}_{24.5}$ , with an average Mg# of 76, and a microprobe analysis on orthopyroxene grains indicated a mostly homogenous major-element chemical composition within crystals, i.e., no first-order zoning (Mori and Takeda, 1981a). Floran et al (1981) analyzed the discrete diopside grains in the matrix and found much higher calcium contents at the expense of both iron and magnesium ( $\text{Wo}_{46.4}\text{En}_{44.4}\text{Fs}_{9.3}$ ), though the grains were reported to be in equilibrium with orthopyroxene.

Orthopyroxenes in Johnstown show thin (<1  $\mu\text{m}$ ) exsolution lamellae, parallel to (100) planes, initially identified as exsolved diopside (Mason, 1963a; Mason and Jarosewich, 1971). Later work recognized these lamellae as pigeonite or augite (Mori and Takeda, 1981a); pigeonite lamellae are usually thicker, with “curtain-like” thin precipitates of augite (Mori and Takeda, 1981a; **Figure 6**), while twinned augite

lamellae up to 20 nm thick are distributed along with abundant one-unit cell wide Guinier-Preston zones (Mori and Takeda, 1981a; Molin et al, 1991; Langenhorst et al, 2006; **Figure 7**) in the orthopyroxene matrix between exsolved pigeonite planes. Guinier-Preston zones are small, Ca-enriched, metastable

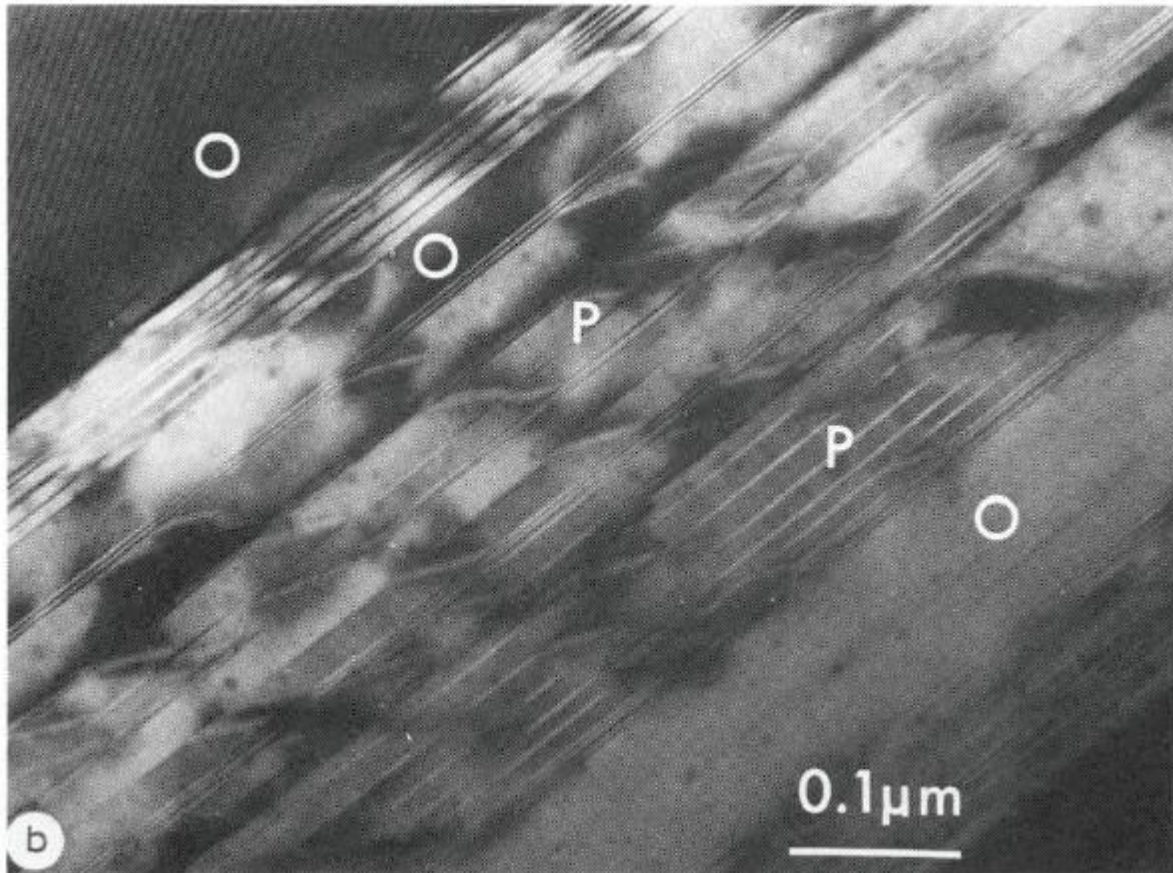


**Figure 6:** Electron micrograph image showing pigeonite lamellae (P) alternating with the host orthopyroxene (O), with curved “curtain-like” augite precipitates at an angle to the pigeonite (100) plane. Mori and Takeda (1981a), Figure 3b.

exsolution phases, parallel to (100), that preceded the formation of more stable augite exsolution lamellae during cooling (Langenhorst et al., 2006).

Merrill and Shannon (*in Hovey*, 1925) also reported (010) twinning in 10% of their separated pyroxenes from Johnstown but this observation has not been confirmed by any other source.

The existence of these exsolution lamellae was first proposed to be related to the high Ca (>1%) content of the orthopyroxenes (Mason, 1963a; Mason and Jarosewich, 1971), which is near the maximum amount that can be incorporated in to the mineral structure; however, chemical analysis showed that there is no appreciable difference in the Ca contents (or that of any major element) of the clinopyroxene lamellae and the orthopyroxene host (Takeda et al, 1982). More recent research (Mori and Takeda, 1981a) has suggested that the augite lamellae and Guinier-Preston zones were the result of rapid cooling from high temperatures followed by slow cooling at lower temperatures, while the pigeonite lamellae were formed from orthopyroxene by a stress-induced transformation at  $\leq 1000^{\circ}\text{C}$ ; these data

indicate the possibility of impact excavation during slow diogenite cooling and crustal development. The orthopyroxene major-element chemistry was likely homogenized by this slow cooling at near-equilibrium conditions in the diogenite pluton body *prior* to any shock-related event (Miyamoto et al, 1975; Mori and Takeda, 1981a; Mittlefehldt, 1994a; see also the discussion of equilibration temperatures, above). A study of Johnstown in conjunction with other diogenitic pyroxenes suggest that

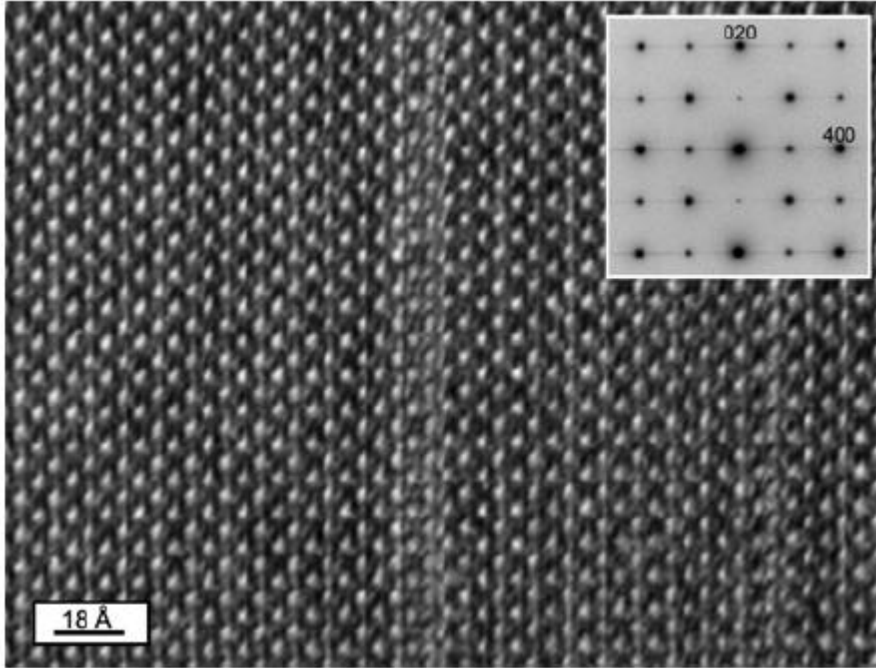
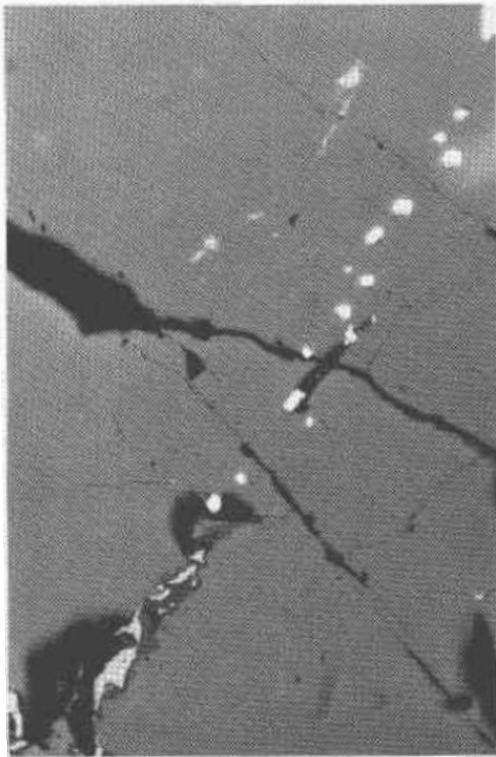


**Figure 7:** High-resolution TEM image of a Guinier-Preston zone in a Johnstown orthopyroxene, with the corresponding electron diffraction pattern, inset. Langenhorst et al (2006), Figure 1. this slow, pre-shock, near-equilibrium cooling may have produced homogenous and unzoned pyroxene crystals to begin with (Takeda, 1979).



Inclusions of chromite, troilite, metal, augite/diopside, and tridymite have also been observed in the orthopyroxenes (first identified as “opaque inclusions” by Merrill and Shannon, *in Hovey*, 1925), mainly oriented in planar arrays at crystal sub-boundaries (Gooley and Moore, 1976; Mori and Takeda, 1981a; **Figure 8**).

Mason and Jarosewich (1971) noted that Johnstown orthopyroxenes are enriched in Cr, as they contain about 5600 ppm Cr (Mason and Graham, 1970), or close to one weight percent (Mason 1963a), versus standard meteoritic orthopyroxenes at 1000 ppm Cr (Mason and Jarosewich, 1971). This may be related to the high temperature of crystallization for Johnstown, though it could also be related to the reduced state of chromium (compatible with the low oxygen fugacity necessary for co-existing free metal), thus allowing greater substitution of Cr for Fe and Mg (Floran et al, 1981).

**Figure 8:** Planar-oriented metal-rich inclusions in a Johnstown orthopyroxene. Other present phases are chromite and tridymite. Gooley and Moore (1976), Figure 1.

There is also a slight deficiency of SiO<sub>2</sub> between the pyroxene chemical analysis and the calculated amount required for a normal pyroxene structure (Mason and Jarosewich, 1971). The orthopyroxene may thus be non-stoichiometric, or some four-coordinated sites (normally occupied by Si) may be occupied by Fe, Cr, or Ti (Mason and Jarosewich, 1971).

Pyroxenes in Johnstown are not the primary REE-bearing phase, as the whole rock and matrix REE values are enriched relative to coarse-grained orthopyroxene (Fukuoka et al, 1977; Mittlefehldt, 1994a; **Figure 9**); while most REE values are sub-chondritic, there is an increase in enrichment from LREEs to HREEs, with a strong negative Eu anomaly (Fukuoka et al, 1977; Fowler et al, 1995).

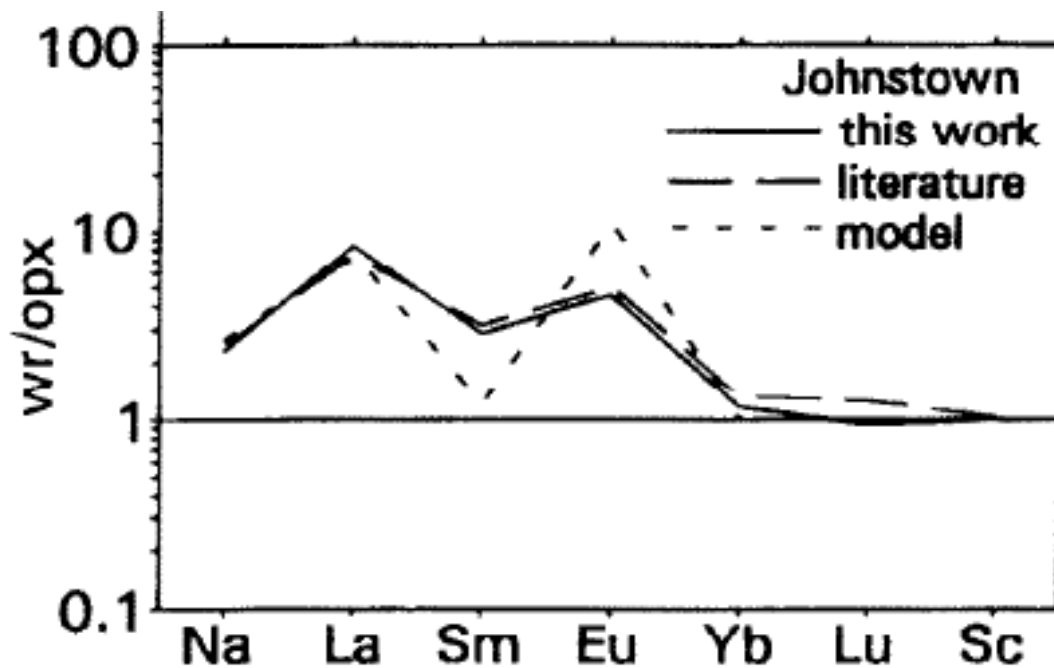


**Figure 9:** Johnstown whole rock and matrix samples normalized to orthopyroxene clasts for REEs and other incompatible lithophile trace elements. Whole rock samples are enriched in the most incompatible elements compared to the clasts (especially La and Eu), indicating that (1) orthopyroxene is not the primary carrier for these elements and (2) whole-rock Johnstown samples likely contain other incompatible element-rich materials mixed in during brecciation. Mittlefehldt (1994a), Figure 3.

**Plagioclase:** Plagioclase feldspar is visible in Johnstown hand samples as sparse, friable “small white spots,” which present in thin section as colorless, inclusion-free crystals (Merrill and Shannon *in Hovey*, 1925) exhibiting albite twinning (some of which are bent by mechanical deformation), primary compositional zoning, and mosaic extinction (Floran et al, 1981). Most crystals are 0.2-0.3 mm (Floran et al, 1981), but a single clast 4 mm in size was analyzed by Mittlefehldt (1979), and its size is suggestive of a deep intrusive crystallization environment. Literature values for plagioclase compositions vary but are centered around An<sub>85-90</sub>, i.e., bytownite (Merrill and Shannon *in Hovey*, 1925; Mason, 1963a; Mason and Jarosewich, 1971; Gooley, 1972; Mittlefehldt, 1979; Floran et al, 1981; Mittlefehldt, 1994a).

Rare earth element patterns in Johnstown plagioclase were analyzed by Mittlefehldt (1979) and Mittlefehldt (1994a), and show enrichment in LREEs (especially La) and a strong positive Eu anomaly relative to chondrites. Similar results were found by Fukuoka et al (1977) for intercumulus material smaller than 150  $\mu\text{m}$ , suggestive of small amounts of plagioclase in the matrix. However, the single plagioclase clast analyzed by Mittlefehldt (1979) was shown to be out of equilibrium with coarse-grained orthopyroxenes such as those analyzed for REEs by Fukuoka et al (1977). It follows that if the plagioclase is not a completely foreign clast, the melt from which plagioclase was formed was probably separated by an extensive crystallization interval from the melt that crystallized orthopyroxene, i.e., the plagioclase may have come from a more fractionated member of the same intrusion as the orthopyroxene (Mittlefehldt, 1979), and was likely mixed in during brecciation.

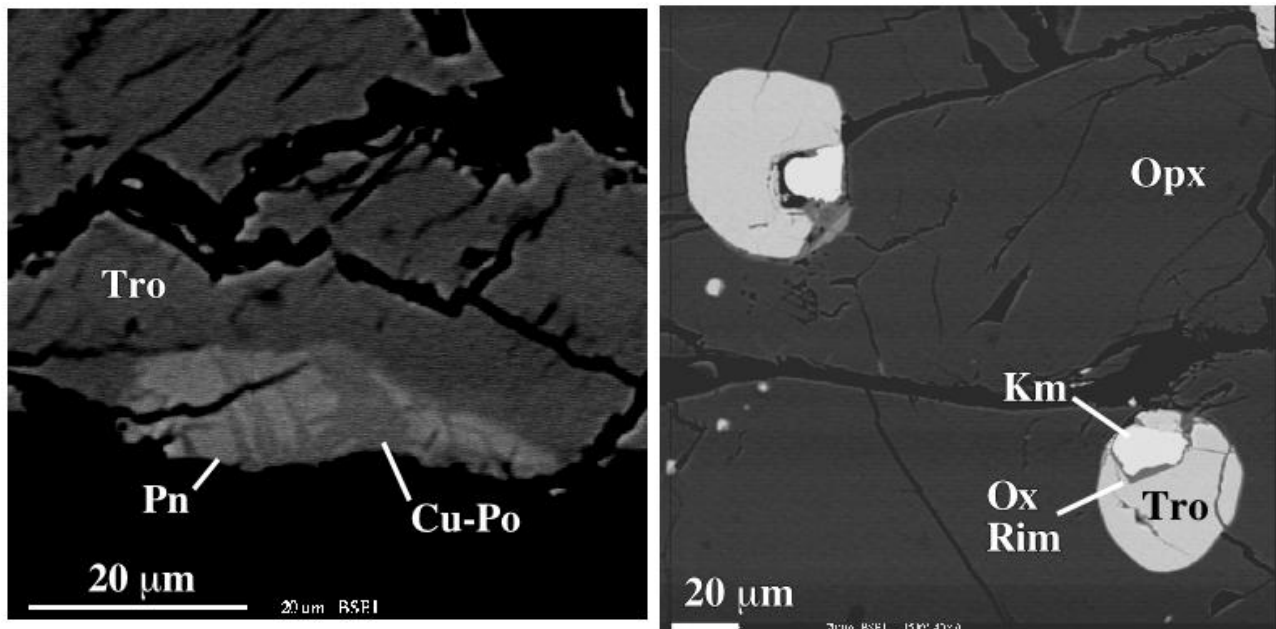


**Figure 10:** Interstitial troilite (left) and troilite included in orthopyroxene (right), with accessory sulfide phases (Pn = pentlandite, Cu-Po = Cu-pyrrhotite, Km = Kamacite). Sideras et al (2004), Figures 1 and 2.

**Chromite:** Chromite generally occurs in conjunction with troilite, tridymite, and metal, as euhedral to subhedral crystals in planar-oriented inclusions in orthopyroxene (Gooley and Moore, 1976; Floran et al, 1981; Sideras et al, 2004) and in anhedral to subhedral patches interstitially in the matrix (Floran et al, 1981; Sideras et al, 2004). Compositionally, Johnstown chromite has an Mg# around 14 (Fredriksson et al, 1976; Mittlefehldt, 1994a) and a Cr# between 80-84 (Bunch and Keil, 1971; Mittlefehldt, 1994a), with average composition  $\text{Cm}_{74.0}\text{Hc}_{6.6}\text{Sp}_{15.1}\text{Mt}_{2.4}\text{Uv}_{1.9}$  (Floran et al, 1981).

**Troilite and other sulfide minerals:** Troilite is primarily found in Johnstown in metal-rich planar-oriented orthopyroxene inclusions (Gooley and Moore, 1976; Floran et al, 1981; Sideras et al, 2004) along with other sulfide minerals such as kamacite, Fe-rich and Ni-rich pentlandites, and Cu-sulfides (Sideras et al, 2004; **Figure 10**). Chemical and textural evidence suggests that sulfide minerals in orthopyroxene inclusions crystallized from an immiscible metal-sulfide melt trapped during crystallization from a magma or later metamorphism (Sideras et al, 2004). Other authors have suggested that sulfide inclusions may also have formed from the reduction of iron from pyroxene coupled with the addition of

sulfur from another source (Gooley and Moore, 1976; Mori and Takeda, 1981a). Troilite also occurs as interstitial matrix grains (Floran et al, 1981).

*Metal:* Though no metal is visible in hand sample (Merrill and Shannon *in Hovey*, 1925), Fe-Ni metal is present in small (0.2-0.3%) modal amounts, as both larger planar-oriented inclusions in pyroxene clasts with troilite, sulfides, chromite, and tridymite, and as discrete matrix grains (Gooley and Moore, 1976; **Figure 8**). Metal particles range in size from less than a micron to 1.3 mm, but the particles in the matrix are usually larger and more irregular in shape (Gooley and Moore, 1976). Chemical analysis of the metal shows mostly Fe (~96%), Ni (2-3%), and Co (0.28-1%), with trace amounts of P, S, and Cu (Hovey, 1925; Merrill and Shannon *in Hovey*, 1925; Gooley and Moore, 1976; Floran et al, 1981). Regardless of differences in Ni and Co abundances between metal inclusions and metal matrix grains, Ni/Co ratios remain the same in all grains; Gooley and Moore (1976) suggest that reduction of Fe from silicates (during metamorphism) would preferentially be incorporated into pre-existing metal particles, diluting their overall composition but retaining their original Ni/Co ratios. Textural relationships in metal-rich inclusions suggest that the metal crystallized first from an immiscible metal-sulfide melt trapped in orthopyroxene crystals during growth, followed by sulfide minerals, chromite, orthopyroxene, diopside, and Ca-phosphate (Sideras et al, 2004); alternatively, metal could have formed from the same Fe reduction that altered the chemistry of any pre-existing metal particles (Gooley and Moore, 1976; Mori and Takeda, 1981a), then migrated and crystallized along annealed fractures (Gooley and Moore, 1976), but there is limited textural evidence for this claim (Sideras et al, 2004).

*Tridymite/Silica:* Tridymite occurs in conjunction with troilite, chromite, and metal in planar-oriented inclusions in orthopyroxene (Gooley and Moore, 1976; Floran et al, 1981; Sideras et al, 2004), and as coarser interstitial grains (up to 0.3 mm in size) associated with troilite and diopside (Floran et al, 1981). Interstitial tridymite is relatively rich in minor oxides, suggesting tridymite as a late-stage residual phase (Floran et al, 1981), while included tridymite may have been excess silica formed either (1) from the reduction of iron in orthopyroxene during metamorphic recrystallization (Gooley and Moore, 1976) or (2) from the latest stage of crystallization of metal-sulfide rich melt inclusions (Sideras et al, 2004).

*Olivine:* Floran et al (1981) reported a single angular fragment of olivine associated with a plagioclase-rich area of Johnstown, with three smaller grains that appeared to have been part of the larger clast at some point. The large fragment, with composition  $Fe_{0.71.3}$ , is fractured, shows undulatory extinction, and is equilibrated relative to the orthopyroxene.

*Phosphates:* Phosphates were identified in Bowman et al (1996) through an automated phase analysis, but in extremely small amounts (0.01%). Sideras et al (2004) reported the existence of Ca-phosphate in metal-rich inclusions in orthopyroxene, occurring in conjunction with troilite, chromite, tridymite, and diopside.

### **Whole Rock Composition:**

The major element chemistry of Johnstown is shown in **Table 2**, followed by minor and trace element data in **Table 3**. An analysis of siderophile element chemistry in Johnstown by Chou et al (1976), showing high contents of iridium, germanium, and gold in similar patterns to howardites, suggested that Johnstown may have been exposed in a regolith and probably contains about 1% chondritic components, similar to mature lunar mare soils. This exposes the possibility that Johnstown is a howardite with a very low percentage of eucritic material (Jerome and Goles, 1971), supported by a

“double-humped” uranium distribution indicating two different sources (i.e. eucrites vs. diogenites) for the uranium in Johnstown (Fisher, 1973). However, textural evidence for this claim is limited.

An investigation of refractory volatiles in HEDs (Mittlefehldt, 1987), though complicated by contamination in Johnstown, indicated the combined effects of fractional crystallization and severe volatile loss in diogenites; some of the low volatile contents, especially Na, may represent equilibration of the diogenitic breccias with plagioclase (Mittlefehldt, 1987).

Whole-rock REE data from **Table 3** is plotted in **Figure 11**, normalized to chondritic values. Mittlefehldt (1994a) noted that the Johnstown samples analyzed for REE by Floran et al (1981) were highly enriched in LREEs; I have included an average of the Floran et al (1981) data here for comparison to the other literature REE values. REE patterns for Johnstown whole-rock samples are very similar to those observed for Johnstown pyroxenes (which would be expected for >95% modal pyroxene), showing progressive increases in REE enrichment from LREEs to HREEs (but still subchondritic), and a strong negative Eu anomaly.

**Figure 11:** Chondrite-normalized REE abundances in Johnstown; chondritic REE values are from Evensen et al (1978).

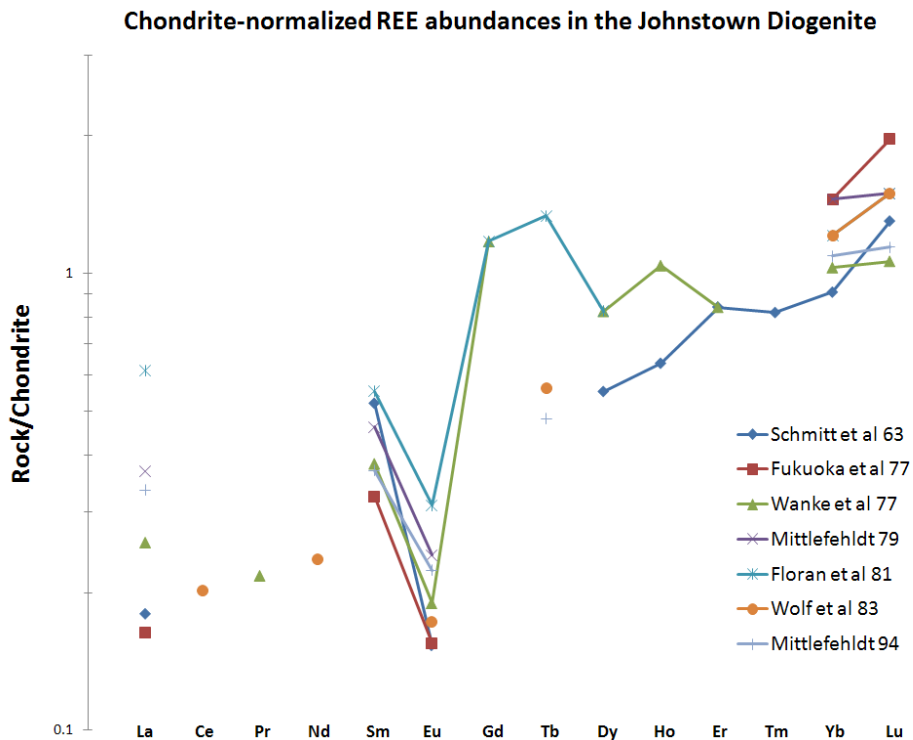


**Table 2: Major element data from the Johnstown diogenite.**

reference	Hovey 25	Urey and Craig 53	Mason and Jarosewich 71	McCarthy et al 72	Fredriksson et al 76	Fukuoka et al 77	Wanke et al 77	Mittlefehldt 79
<i>weight</i>	--	--	8.5 g	21.8 g	--	500 mg	--	797.4 mg
<i>SiO<sub>2</sub></i>	50.31	49.83	53.48	53.63	53.4	--	52.5	--
<i>TiO<sub>2</sub></i>	--	--	0.12	0.12	0.14	0.12	0.11	0.22
<i>Al<sub>2</sub>O<sub>3</sub></i>	2.352	2.33	1.43	1.23	1.24	1.38	1.49	1.67
<i>FeO</i>	15	13.64	15.63	16.26	16	15.9	15.91	17.69
<i>MnO</i>	0.4	0.4	0.54	0.5	0.52	0.47	0.48	0.52
<i>MgO</i>	26.88	26.62	25.87	25.9	26.7	27.1	25.47	27.36
<i>CaO</i>	2.63	2.61	1.4	1.46	1.52	1.3	1.83	1.4
<i>Na<sub>2</sub>O</i>	0.33	0.33	0.04	0.03	0.04	<0.01	--	0.06
<i>K<sub>2</sub>O</i>	0.1	0.1	0	0.002	0.05	<0.002	--	0.002
<i>Cr<sub>2</sub>O<sub>3</sub></i>	2.02	1	0.83	0.86	0.88	0.8	--	0.9
<i>P<sub>2</sub>O<sub>5</sub></i>	--	0.03	0	0.014	--	--	<i>Gibson et al 85</i>	--
<i>S%</i>	--	0.57	--	--	--	--	0.313	--
<i>H<sub>2</sub>O+</i>	--	--	<0.1	--	--	--	--	--
<i>H<sub>2</sub>O-</i>	--	--	0.05	--	--	--	--	--
<i>Fe (met)</i>	0.88	0.87	--	--	--	--	--	--
<i>FeS</i>	1.168	1.55	1.18	--	1.1	--	--	--
<i>SO<sub>3</sub></i>	0.868	--	--	--	--	--	--	--
<b>sum</b>	<b>100.003</b>	<b>99.31</b>	<b>100.57</b>	--	<b>101.6</b>	--	--	--
<i>technique:</i>	wet chem	lit. survey	wet chem	XRF	EPMA	INAA	INAA	INAA

reference	Jochum et al 80	Floran et al 81 average of 7 analyses	Mittlefehldt 94a	Welten et al 97a	Genge and Grady 99 fusion crust	AVERAGE LIT VALUES
<i>weight</i>	--	--	--	--	--	--
<i>SiO<sub>2</sub></i>	54.55	53.06	--	52.84	52.92	<b>52.65</b>
<i>TiO<sub>2</sub></i>	--	0.13	--	0.12	0.13	<b>0.14</b>
<i>Al<sub>2</sub>O<sub>3</sub></i>	1.51	1.32	--	0.96	1.4	<b>1.53</b>
<i>FeO</i>	18.27	15.95	15.7	15.18	18.86	<b>16.15</b>
<i>MnO</i>	0.54	0.48	--	0.5	0.51	<b>0.49</b>
<i>MgO</i>	26.2	25.21	--	25.54	24.15	<b>26.08</b>
<i>CaO</i>	1.68	1.45	1.5	1.18	1.33	<b>1.64</b>
<i>Na<sub>2</sub>O</i>	--	--	0.02	--	--	<b>0.12</b>
<i>K<sub>2</sub>O</i>	--	--	0.01	0.001	--	<b>0.03</b>
<i>Cr<sub>2</sub>O<sub>3</sub></i>	1	0.83	0.8	0.5	0.55	<b>0.91</b>
<i>P<sub>2</sub>O<sub>5</sub></i>	--	--	--	--	--	<b>0.01</b>
<i>S%</i>	0.35	--	--	0.12	--	<b>0.34</b>
<i>H<sub>2</sub>O+</i>	--	--	--	--	--	<b>&lt;0.1</b>
<i>H<sub>2</sub>O-</i>	--	--	--	--	--	<b>0.05</b>
<i>Fe (met)</i>	--	--	--	--	--	<b>0.88</b>
<i>FeS</i>	--	--	--	--	--	<b>1.25</b>
<i>SO<sub>3</sub></i>	--	--	--	--	--	<b>0.87</b>
<b>sum</b>	--	--	--	--	<b>99.85</b>	--
<i>technique:</i>	spark source MS	XRF, INAA, RNAA	INAA	ICPMS	EPMA	--

**Table 3: Minor and trace element data from the Johnstown diogenite.**

reference weight comments	Mittlefehldt 79 797.4 mg	Floran et al 81 avg. of 7 analyses	Wolf et al 83 245 mg	Mittlefehldt 87	Mittlefehldt 94a 46.35 mg
Ca ppm	10000 (c)	--	--	--	--
Na ppm	410 (c)	183.43 (c,d,e)	--	137 (a)	175 (c)
K ppm	14 (c)	16.86 (c,d,e)	--	37 (a)	97 (c)
P ppm	--	--	--	97 (a)	--
Sc ppm	16.2 (c)	16.01 (c,d,e)	18 (d)	--	15 (c)
Ti ppm	1300 (c)	--	--	--	--
V ppm	119 (c)	--	--	--	--
Cr ppm	6190 (c)	--	6890 (d)	--	--
Mn ppm	4000 (c)	--	--	--	--
Co ppm	36.9 (c)	27.29 (c,d,e)	--	<i>Chou et al 76</i>	25.7 (c)
Ni ppm	190 (c)	106 (c,d,e)	67.85 (d)	172 (d)	110 (c)
Cu ppm	--	--	--	--	--
Zn ppm	--	--	0.71 (d)	0.71 (d)	--
Ga ppm	--	--	--	0.22 (d)	--
Ge ppm	--	--	0.056 (d)	0.022 (d)	--
As ppb	--	258.75 (c,d,e)	--	--	300 (c)
Se ppm	1.8 (c)	--	0.433 (d)	<i>Mittlefehldt 87</i>	0.4 (c)
Rb ppm	--	--	0.03 (d)	0.042 (a)	--
Sr ppm	--	--	--	--	--
Y ppm	--	--	--	--	--
Zr ppm	--	--	--	--	--
Nb ppm	--	--	--	--	--
Mo ppb	--	--	--	<i>Chou et al 76</i>	--
Ru ppm	--	--	--	0.015 (d)	--
Rh ppm	--	--	--	--	--
Pd ppb	--	--	1.86 (d)	--	--
Ag ppb	--	--	11.40 (d)	<i>Chou et al 76</i>	--
Cd ppb	--	--	20.50 (d)	7 (d)	--
In ppb	--	--	3.19 (d)	0.38 (d)	--
Sn ppb	--	--	--	--	--
Sb ppb	--	--	11.25 (d)	--	--
Te ppb	--	--	4.96 (d)	<i>Mittlefehldt 87</i>	--
Cs ppb	--	--	1.1 (d)	1.1 (a)	--
Ba ppm	--	--	--	--	--
La ppm	0.09 (c)	0.15 (c,d,e)	--	--	0.082 (c)
Ce ppm	--	--	0.129 (d)	--	--
Pr ppm	--	--	--	--	--
Nd ppm	--	--	0.112 (d)	--	--
Sm ppm	0.07 (c)	0.085 (c,d,e)	--	--	0.057 (c)
Eu ppm	0.014 (c)	0.018 (c,d,e)	0.010 (d)	--	0.013 (c)
Gd ppm	--	0.24 (c,d,e)	--	--	--
Tb ppm	--	0.055 (c,d,e)	0.021 (d)	--	0.018 (c)
Dy ppm	--	0.21 (c,d,e)	--	--	--
Ho ppm	--	--	--	--	--
Er ppm	--	--	--	--	--
Tm ppm	--	--	--	--	--
Yb ppm	0.24 (c)	0.2 (c,d,e)	0.2 (d)	--	0.18 (c)
Lu ppm	0.038 (c)	0.038 (c,d,e)	0.038 (d)	<i>Shima 79</i>	0.029 (c)
Hf ppb	--	--	--	182 (g)	50 (c)
Ta ppb	--	--	--	--	--
W ppb	--	--	--	--	--
Re ppb	--	--	0.15 (d)	--	--
Os ppb	--	--	2.02 (d)	<i>Chou et al 76</i>	--
Ir ppb	9.6 (c)	6.13 (c,d,e)	2.04 (d)	6.8 (d)	--
Pt ppb	--	--	--	--	--
Au ppb	2.1 (c)	26.07 (c,d,e)	1.88 (d)	<i>Morgan and Lovering 73</i>	2.8 (c)
Th ppb	--	--	--	11.6 (d)	--
U ppb	--	--	1.9 (d)	30 (d)	--
Li ppm	--	--	--	--	--
Be ppm	--	--	--	--	--
B ppm	--	--	--	--	--
S ppm	--	--	--	--	--
F ppm	--	--	--	--	--
Cl ppm	--	--	--	--	--
Br ppm	--	0.23 (c,d,e)	--	--	0.12 (c)
I ppb	--	--	--	--	--
Pb ppm	--	--	--	--	--
Hg ppb	--	--	--	--	--
Tl (ppb)	--	--	2.38 (d)	--	--
Bi (ppb)	--	--	0.18 (d)	--	--

technique: (a) literature survey, (b) wet chemistry, (c) INAA, (d) RNAA, (e) XRF, (f) spark source MS, (g) surface ionization source MS

**Table 3, continued:** Minor and trace element data from the Johnstown diogenite.

reference weight	Mason 63a	Mason and Jarosewich 71 8.5 g	McCarthy et al 72 21.8 g	Fukuoka et al 77 500 mg	Wanke et al 77
comments	incl. other sources	incl. other sources			
Ca ppm	--	10000 (b)	--	--	--
Na ppm	--	300 (b)	--	--	150 (c)
K ppm	10 (a)	9.9 (a)	20 (e)	--	9.2 (c)
P ppm	--	--	--	--	180 (c)
Sc ppm	14 (a)	41 (a)	<i>Shima 79</i>	15.0 (c)	15.8 (c)
Ti ppm	--	720 (b)	<i>802 (g)</i>	--	--
V ppm	--	--	--	105 (c)	115 (c)
Cr ppm	3200 (a)	5700 (b)	--	--	5610 (c)
Mn ppm	--	4200 (b)	--	--	3750 (c)
Co ppm	--	--	--	29 (c)	38.1 (c)
Ni ppm	--	--	90 (e)	120 (c)	150 (c)
Cu ppm	--	7 (a)	--	--	4.2 (c)
Zn ppm	3 (a)	3 (a)	--	--	0.65 (c)
Ga ppm	--	--	--	--	0.18 (c)
Ge ppm	--	--	--	--	0.13 (c)
As ppb	--	--	--	--	32 (c)
Se ppm	0.007 (a)	--	--	--	--
Rb ppm	0.105 (a)	0.139 (a)	--	--	--
Sr ppm	3 (a)	2.07 (a)	<2 (e)	--	--
Y ppm	1.22 (a)	1.22 (a)	<2 (e)	--	--
Zr ppm	30 (a)	1.9 (a)	<2 (e)	--	<1 (c)
Nb ppm	--	--	--	--	<5 (c)
Mo ppb	--	--	--	--	--
Ru ppm	--	--	--	--	--
Rh ppm	--	--	--	--	--
Pd ppb	--	--	--	--	--
Ag ppb	--	--	--	--	--
Cd ppb	--	330 (a)	--	--	--
In ppb	--	--	--	--	--
Sn ppb	--	--	--	--	--
Sb ppb	--	--	--	--	--
Te ppb	7 (a)	--	--	--	--
Cs ppb	7 (a)	7.6 (a)	--	--	--
Ba ppm	5 (a)	2.5 (a)	<2 (e)	--	--
La ppm	0.044 (a)	0.044 (a)	--	0.04 (c)	0.063 (c)
Ce ppm	--	0.4 (a)	--	--	--
Pr ppm	--	--	--	--	0.021 (c)
Nd ppm	--	--	--	--	--
Sm ppm	0.08 (a)	0.08 (a)	--	0.050 (c)	0.059 (c)
Eu ppm	0.0089 (a)	0.0089 (a)	--	0.009 (c)	0.011 (c)
Gd ppm	--	--	--	--	0.24 (c)
Tb ppm	--	--	--	--	--
Dy ppm	0.14 (a)	0.14 (a)	--	--	0.21 (c)
Ho ppm	0.036 (a)	0.036 (a)	--	--	0.059 (c)
Er ppm	0.14 (a)	0.14 (a)	--	--	0.14 (c)
Tm ppm	0.021 (a)	0.021 (a)	--	--	--
Yb ppm	0.15 (a)	0.15 (a)	--	0.024 (c)	0.17 (c)
Lu ppm	0.033 (a)	0.033 (a)	--	0.05 (c)	0.027 (c)
Hf ppb	--	40 (a)	--	--	--
Ta ppb	8 (a)	8 (a)	<i>Hintenberger et al 73</i>	--	--
W ppb	6 (a)	--	200 (f)	--	3.5 (c)
Re ppb	--	--	21 (f)	--	--
Os ppb	--	--	38 (f)	--	--
Ir ppb	8 (a)	--	17 (f)	--	6.4 (c)
Pt ppb	--	--	19 (f)	--	--
Au ppb	--	--	4 (f)	<5 (c)	1.7 (c)
Th ppb	5.9 (a)	5.9 (a)	32 (f)	--	--
U ppb	2.2 (a)	2.2 (a)	26 (f)	--	2.8 (c)
Li ppm	--	--	--	--	2.7 (c)
Be ppm	<i>Curtis et al 80</i>	--	--	--	--
B ppm	5.1	<i>Gibson et al 85</i>	--	--	--
S ppm	--	3130	--	--	2200 (c)
F ppm	--	--	--	--	2 (c)
Cl ppm	--	--	--	--	5.5 (c)
Br ppm	--	--	--	--	0.051 (c)
I ppb	--	--	<i>Hintenberger et al 73</i>	--	0.017 (c)
Pb ppm	--	--	4.37 (f)	--	--
Hg ppb	--	--	2480 (f)	--	--
Tl (ppb)	--	--	5.8 (f)	--	--
Bi (ppb)	--	--	8.9 (f)	--	--

(REE and trace element data from Schmitt et al 62, Schmitt et al 63)

technique: (a) literature survey, (b) wet chemistry, (c) INAA, (d) RNAA, (e) XRF, (f) spark source MS, (g) surface ionization source MS

**Radiogenic Isotopes:** Literature values for Johnstown age dates are somewhat sparse; no U-Th-Pb, Pb-Pb, Sm-Nd, Hf-W, or Pu-Xe dates could be found in the literature for Johnstown.

The first reported K-Ar age for Johnstown, 4.32 Ga, was published by Kirsten et al (1963); this was revised by Megrue (1968), who reported a much more recent value of 3.2 Ga as the latest date of differentiation and cooling below 600°C. Ar-Ar plateau ages (reported by Balacescu and Wanke, 1977) give values around 3.7 Ga; clearly the K-Ar system has experienced resetting due to later metamorphism (such as shock or impact effects).

Birck and Allegre (1981) analyzed Johnstown and other diogenites for Rb-Sr ages; when the diogenite whole-rock values are plotted together on a single isochron, their Rb-Sr age is  $4.45 \pm 0.18$  Ga, and when the diogenites are plotted with eucrites their Rb-Sr age is  $4.47 \pm 0.10$  Ga. Later Rb-Sr work (Takahashi and Masuda, 1990) showed that Johnstown point data describe a different isochron than those of eucrites such as Juvinas, giving an Rb-Sr age of  $4.394 \pm 0.011$  Ga (**Figure 12**).

Mn-Cr systematics in Johnstown were investigated by Lugmair and Shukolyukov (1998) and Trinquier et al (2008); together with other eucrites and diogenites, Johnstown helps define an isochron of  $4564.8 \pm 0.9$  Ga (Lugmair and Shukolyukov, 1998) or  $4564.9 \pm 1.1$  Ga (Trinquer et al, 2008) for the last Mn/Cr fractionation in the HED parent body mantle.  $^{55}\text{Mn}/^{52}\text{Cr}$  ratios and  $\epsilon_{53\text{Cr}}$  were also measured by both authors (Lugmair and Shukolyukov, 1998:  $^{55}\text{Mn}/^{52}\text{Cr} = 0.73$ ,  $\epsilon_{53\text{Cr}} = 0.58 \pm 0.09$ ; Trinquer et al, 2008:  $^{55}\text{Mn}/^{52}\text{Cr} = 0.64$ ,  $\epsilon_{53\text{Cr}} = 0.18 \pm 0.06$ ), and the sub-chondritic nature of these values is consistent with volatile Mn fractionation relative to Cr.

**Cosmogenic Isotopes:** Literature values for cosmogenic exposure ages are contained in **Table 4**, below. Each source contains further information on the isotopic composition of each noble gas, and other sources where more information is available.

**Table 4:** Noble-gas exposure ages for Johnstown. All ages are in millions of years.

source	Megrue 68 whole rock	Megrue 68 opx	Fuse and Anders 69 whole rock	Herzog and Cressy 77 whole rock	Welten et al 97a whole rock	Seitz et al 07 whole rock	Seitz et al 07 opx
Ages							
$^3\text{He}$	22	23	19.4	16.7	23	28	28
$^{21}\text{Ne}$	18	19		13.1	21.8		
$^{38}\text{Ar}$	22	20		13.7	24.3		
$^{26}\text{Al}$			23				
<b>Average</b>	<b>20.67</b>	<b>20.67</b>	<b>21.20</b>	<b>14.50</b>	<b>22.9 ± 0.9</b>	<b>28.00</b>	<b>28.00</b>

**Other Isotopes:**

**Oxygen:** Taylor et al (1965) measure oxygen isotopes in a variety of meteorites, and found that the  $\delta^{18}\text{O}$  values for Johnstown ( $3.7 \pm 0.1\text{‰}$  for pyroxene and  $3.7 \pm 0.1\text{‰}$  calculated for the whole rock) coincided

with those for other basaltic achondrites, hypersthene achondrites, and mesosiderites (all ranging from 3.7-4.4‰), suggesting a common parent body. Oxygen isotopes were measured in two Johnstown

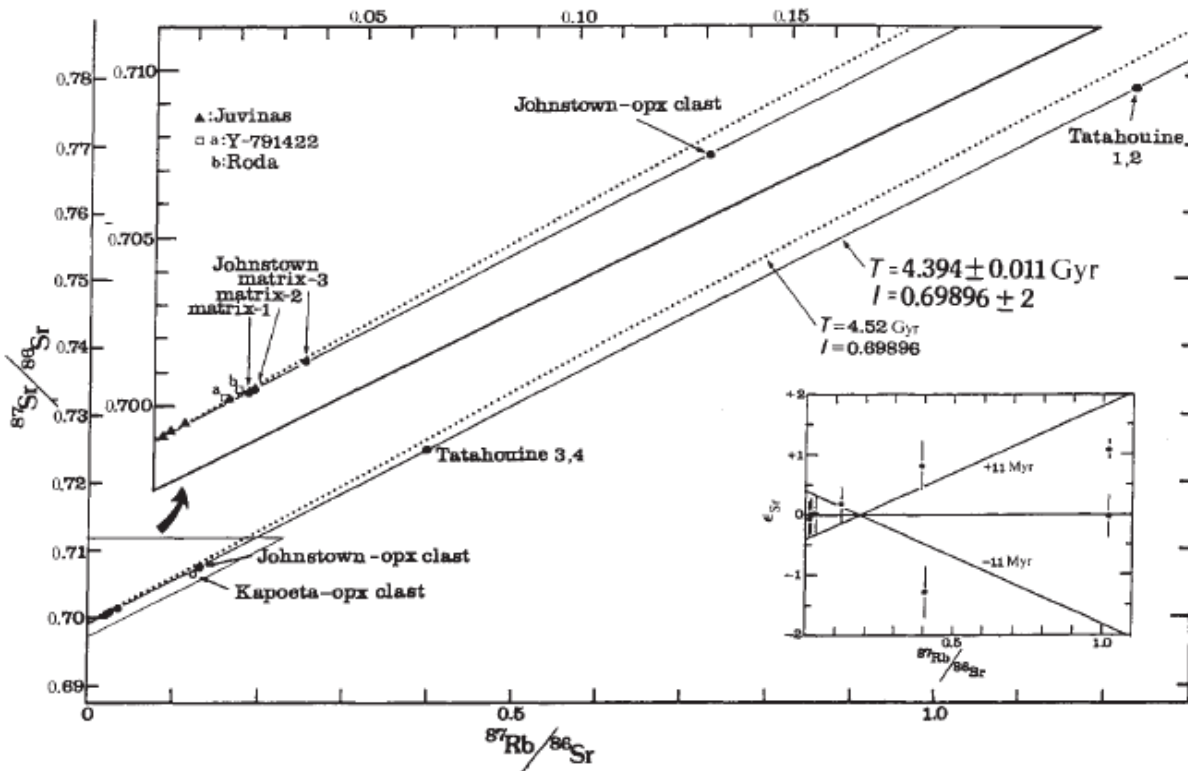


**Figure 12:** Johnstown (and Tatahouine) Rb/Sr isochron (solid line) plotted next to Juvinas isochron (dotted line), showing an age of  $4.394 \pm 0.011 \text{ Ga}$ . Takahashi and Masuda (1990), Figure 1.

fragments, one brecciated and one unbrecciated, by Wiechert et al (2004), who measured  $\delta^{18}\text{O}$  (unbrecciated) = 3.331‰,  $\delta^{18}\text{O}$  (brecciated) = 3.473‰,  $\delta^{17}\text{O}$  (unbrecciated) = 1.534‰,  $\delta^{17}\text{O}$  (brecciated) = 1.624‰, and values of  $\Delta^{17}\text{O}$  at  $-0.233 \pm 0.016$  and  $-0.219 \pm 0.014$ , falling within the ranges that were measured for overall HEDs. Another oxygen isotope study (Greenwood et al, 2005) found very similar  $\delta^{18}\text{O}$  ( $3.497\% \pm 0.154\%$ ),  $\delta^{17}\text{O}$  ( $1.602\% \pm 0.104\%$ ) and  $\Delta^{17}\text{O}$  ( $-0.231 \pm 0.026$ ) values, again falling within the HED values measured in the same study.

**Carbon:** Grady et al (1997) examined C isotopes in Johnstown, and found an overall concentration of 250 ppm, with  $\delta^{13}\text{C} = -25\%$ ; however, most of this carbon was assumed to be terrestrial, and the sample was heated to  $600^\circ\text{C}$  to measure the indigenous C value, which is much less (27 ppm,  $\delta^{13}\text{C} = -27\%$ ). These  $\delta^{13}\text{C}$  values are similar to other diogenites and eucrites, as well as lunar and Martian samples, but less than terrestrial values (Grady et al, 1997).

**Beryllium:** A  $^{10}\text{Be}$  content of  $26.3 \pm 2.8 \text{ dpm/kg}$  was measured in Johnstown by Moniot et al (1982).

**Lithium:** Seitz et al (2007) analyzed lithium isotopic concentrations in a variety of meteoritic materials; the Johnstown whole rock  $\delta^7\text{Li}$  value ( $3.5\% \pm 0.5\%$ ) falls well within the overall HED range (3.0-4.7%).

*Aluminum:*  $^{26}\text{Al}$  depletion rates were investigated by Fuse and Anders (1969) ( $67.2 \pm 2.4$  dpm/kg), and Lavrukhina and Ustinova (1972) used this value to calculate the aphelion of Johnstown.

*Iron:* Iron isotopes were analyzed in a variety of planetary materials by Poitrasson et al (2004); Johnstown values ( $\delta^{57}\text{Fe}/^{54}\text{Fe} = 0.053\text{‰} \pm 0.084\text{‰}$ ,  $\delta^{57}\text{Fe}/^{56}\text{Fe} = -0.043\text{‰} \pm 0.038\text{‰}$ ) fit well within the mean for HED samples, which in turn are identical to Martian meteorites (within error), but lighter than terrestrial or lunar samples, suggesting different processes of planetary formation.

*Magnesium:* Mg isotope values in Johnstown ( $\delta^{26}\text{Mg}_{\text{DSM3}} = -0.38\text{‰} \pm 0.04\text{‰}$ ,  $\delta^{26}\text{Mg}_{\text{DSM3}} = -0.16\text{‰} \pm 0.03\text{‰}$ ,  $\Delta^{25}\text{Mg} = 0.040\text{‰} \pm 0.016\text{‰}$ ; Wiechert and Halliday, 2007) are lighter than those found in eucrites and most terrestrial samples, but similar to lunar and chondritic values; regardless, all measured values plot on a single fractionation curve, suggesting a single homogenous Mg reservoir for the solar system.

**Experiments:** A significant body of work, both theoretical and experimental, has been developed on Fe-Mg order/disorder, closure temperatures, and cooling rates in Johnstown pyroxenes, most of which is beyond the scope of this paper; for more information, including references to other similar work, see Miyamoto et al (1975), Mori and Takeda (1981a), Mukherjee and Viswanath (1987), Molin et al (1991), Mittlefehldt (1994a), Zema et al (1997), and Heinemann et al (2000). As a corollary, Goswami et al (1984) used a hypersthene from Johnstown to experimentally model critical temperatures and other parameters for the annealing of cosmic-ray and heavy nuclide particle tracks.

Petrogenetic constraints and models for the HED parent body, based on major and minor element data from Johnstown (and other HED meteorites), were determined by Mittlefehldt (1979), Grove and Bartels (1992), Mittlefehldt (1994a), Fowler et al (1994), and Fowler et al (1995).

Magnetic anisotropy in Johnstown was quantified by Collinson and Morden (1994), Gattacceca et al (2005), and Gattacceca et al (2008); an analysis of natural remnant magnetization in Collinson and Morden (1994) concluded that Johnstown has both primary and secondary NRM, the latter of which may have been formed during collisional events.

Thermoluminescence was examined and discussed for Johnstown by Batchelor and Sears (1991) and Sears et al (1991). Diogenitic meteorites as a group show lower TL intensity than other basaltic meteorites because of the lower fraction of plagioclase (Batchelor and Sears, 1991), and TL data from plagioclase in these rocks suggests metamorphic equilibration temperatures were  $\leq 800^\circ\text{C}$  after igneous processing (Batchelor and Sears, 1991).

Various other measured spectra are available in the literature for Johnstown, including visible reflectance spectra (Salisbury et al, 1991; Hiroi and Pieters, 1998; Shestopalov et al, 2008), luminescence spectra (Geake and Walker, 1966), and thermal release profiles of volatile trace metals (Cirlin and Housley, 1978).

Oxygen fugacity in Johnstown was quantified by Gooley and Moore (1976) and Hewins and Ulmer (1984); the results from Gooley and Moore (1976) plot at one log unit below the iron-wüstite buffer, whereas the Hewins and Ulmer (1984) values are one log unit *above*. The discrepancy may have resulted from the Williams (1971) method used by Gooley and Moore (1976) to calculate  $f\text{O}_2$ , which assumes

equilibrium between olivine, orthopyroxene, and metal that may never have been the case in Johnstown (Hewins and Ulmer, 1984), especially if the metal formed by reduction of Fe from pyroxene (Gooley and Moore, 1976; Mori and Takeda, 1981a).

**Metamorphism and Shock Effects:** Most evidence for metamorphism in Johnstown is preserved in pyroxenes, which exhibit augite exsolution lamellae, Guinier-Preston zones,  $120^\circ$  triple-grain boundaries in orthopyroxenite clasts, planar opaque inclusions, equilibrated compositions between *and* within clasts, and a lack of major-element zoning, suggestive of some sort of thermal metamorphism or slow sub-solidus cooling *before* brecciation (Mason, 1963a; Floran et al, 1981; Mori and Takeda, 1981a; Molin et al, 1991; Mittlefehldt, 1994a). TL data on plagioclase (Batchelor and Sears, 1991) suggests that diogenites were metamorphosed at  $\leq 800^\circ\text{C}$  after initial crystallization; however, Johnstown plagioclase shows evidence of primary compositional zoning (Floran et al, 1981), which is consistent with the idea that plagioclase came from a more-fractionated and evolved (and perhaps less metamorphosed) member of the same intrusion as the pyroxene, and was only mixed in during later brecciation (Mittlefehldt, 1979). Some thermometry data from pyroxene (Miyamoto et al, 1975) suggests slow cooling in the  $500\text{-}700^\circ\text{C}$  range, but more recent work has calculated equilibration temperatures closer to  $650\text{-}700^\circ\text{C}$  (Mukherjee and Viswanath, 1987; Mittlefehldt, 1994a).

Shock textures in Johnstown include shock-induced pigeonite lamellae in pyroxene (Mori and Takeda, 1981a), undulatory pyroxene extinction (Mason, 1963a; Floran et al, 1981), numerous fractures in orthopyroxene (Floran et al, 1981), bent albite twins in plagioclase (Floran et al, 1981), and mosaic plagioclase extinction (Floran et al, 1981); resetting of certain age-dating systems may also be related to impact and shock effects.